Macromolecular Bioscience
www.mbs-journal.de

Imaging the In Vivo Degradation of Tissue Engineering Implants by Use of Supramolecular Radiopaque Biomaterials

Hanna Talacua, Serge H. M. Söntjens, Shraddha H. Thakkar, Aurelie M. A. Brizard, Lex A. van Herwerden, Aryan Vink, Geert C. van Almen, Patricia Y. W. Dankers, Carlijn V. C. Bouten, Ricardo P. J. Budde, Henk M. Janssen, and Jolanda Kluin*

For in situ tissue engineering (TE) applications it is important that implant degradation proceeds in concord with neo-tissue formation to avoid graft failure. It will therefore be valuable to have an imaging contrast agent (CA) available that can report on the degrading implant. For this purpose, a biodegradable radiopaque biomaterial is presented, modularly composed of a bisurea chain-extended polycaprolactone (PCL2000-U4U) elastomer and a novel iodinated bisurea-modified CA additive (I-U4U). Supramolecular hydrogen bonding interactions between the components ensure their intimate mixing. Porous implant TE-grafts are prepared by simply electrospinning a solution containing PCL2000-U4U and I-U4U. Rats receive an aortic interposition graft, either composed of only PCL2000-U4U (control) or of PCL2000-U4U and I-U4U (test). The grafts are explanted for analysis at three time points over a 1-month period. Computed tomography imaging of the test group implants prior to explantation shows a decrease in iodide volume and density over time. Explant analysis also indicates scaffold degradation. (Immuno)histochemistry shows comparable cellular contents and a similar neo-tissue formation process for test and control group, demonstrating that the CA does not have apparent adverse effects. A supramolecular approach to create solid radiopaque biomaterials can therefore be used to noninvasively monitor the biodegradation of synthetic implants.

1. Introduction

In situ tissue engineering (TE) represents a promising new therapeutic option for cardiovascular diseases and has been suggested to overcome shortcomings of currently used prostheses.[1–3] In this TE approach, a cell-free degradable scaffold is implanted, and in vivo cell repopulation is intended. Cells differentiate at the implantation site where subsequently neo-tissue is formed in vivo.[4–6] While neo-tissue is formed, the scaffold degrades, and ultimately a native autologous substitute remains.[7] In situ cardiovascular TE approaches place high demands on the properties of the scaffold implant. The scaffold should be a highly porous, non-thrombogenic and biodegradable matrix, so that a 3D template is provided for cell adhesion, cell differentiation and tissue generation.[8] Initially, the cardiovascular implant should be able to bear all the mechanical loads and strains placed upon it, and over time the scaffold should safely

Dr. H. Talacua, Prof. L. A. van Herwerden, Prof. J. Kluin
Department of Cardiothoracic Surgery
University Medical Center Utrecht
Heidelberglaan 100, Utrecht, The Netherlands
Dr. H. Talacua, Prof. J. Kluin
Department of Cardio-Thoracic Surgery
Academic Medical Center Amsterdam
P. O. Box 22660, Amsterdam 1100 DD, The Netherlands
Dr. S. H. M. Söntjens, Dr. H. M. Janssen
SyMO-Chem BV, Eindhoven
Den Dolech 2, Eindhoven, The Netherlands
The ORCID identification number(s) for the author(s) of this article can be found under https://doi.org/10.1002/mabi.202000024.

DOI: 10.1002/mabi.202000024

Dr. S. H. Thakkar, Prof. C. V. C. Bouten
Department of Biomedical Engineering
Laboratory of Cell and Tissue Engineering
Eindhoven University of Technology
Den Dolech 2, Eindhoven, The Netherlands
Dr. A. M. A. Brizard
Philips Research
BioMolecular Engineering
High Tech Campus Eindhoven
High Tech Campus 11, Eindhoven, The Netherlands
Dr. A. Vink
Department of Pathology
University Medical Center Utrecht
Heidelberglaan 100, Utrecht, Room H04-312, Utrecht, The Netherlands
Dr. G. C. van Almen, Prof. P. Y. W. Dankers
Department of Biomedical Engineering
Laboratory of Chemical Biology
Eindhoven University of Technology
Den Dolech 2, Eindhoven, The Netherlands
E-mail: p.y.w.dankers@tue.nl

degrade and disappear. A timely and controlled degradation of the scaffold is a key element in in situ TE, as there has to be a balance between in vivo tissue formation and scaffold degradation. If the scaffold degrades before sufficient load bearing tissue is formed, failure of the scaffold implant occurs with disastrous consequences. Accordingly, it would be valuable to be able to noninvasively image and monitor the degradation of implanted biomaterials in situ. For this, an imaging CA is required that can report on the status and fate of the (degrading) implant as a whole, and not merely on the CA itself.

Currently, the scope of noninvasive imaging in TE is mainly focused on tracking cells, on characterizing tissue response and on monitoring the function or patency of implants. Only a limited number of reports show the direct in vivo visualization of the degradation of solid organic material implants suitable for in situ cardiovascular TE.[9–11] Furthermore, in other research, collagen scaffolds labeled with ultrasmall superparamagnetic iron oxide (USPIO) nanoparticles have been studied and implanted subcutaneously,[12] and poly(vinylidene fluoride) (PVDF)-based textile fibers combined with USPIOs have been surgically implanted into sheep as arteriovenous shunts after a bioreactor cultivation step.[13] Both systems could be imaged with MRI, but for the collagen scaffolds no degradation was observed, and for the PVDF-USPIO scaffolds no degradation is to be expected, as PVDF is nonbiodegradable. Various researchers have been successful in imaging the in vivo degradation of polyester,[14–16] polyurethane-urea,[17,18] or collagen[19] scaffold implant materials, and have mainly used ultrasound elasticity imaging (UEI), but also ultrasound shear wave imaging (USWI), photoacoustic imaging and microscopy (PAI and PAM), and near-infrared fluorescence (NIRF) imaging.[9–11] All these techniques are very valuable, but also have drawbacks. For instance, UEI imaging requires that physical compression can be easily applied to the areas of interest, and NIRF imaging has a limited penetration depth.

In this study we have chosen the widely applied computed tomography (CT) as the noninvasive imaging technique to monitor implant degradation. CT contrast agents (CAs) are always based on high-Z (heavy) elements, such as iodine or barium, and are commonly used clinically. Water soluble iodinated CAs are applied intravascularly to acquire arterial and venous angiograms, and also oil based CAs (e.g., Lipiodol) are known,[20–22] but neither of these two classes of CA are suitable for monitoring implant degradation in vivo, as both types of CA presumably give a fast leakage out of the biomaterial implant.

A variety of radiopaque polymeric CAs for various uses have been developed and reported.[23] For instance, highly radiopaque salts or elements can be mixed-in with polymers, but this approach will have the disadvantage that materials become inhomogeneous and may suffer from deteriorated mechanical properties. Furthermore, most radiopaque salts or elements do not biodegrade, and remain in the body after implantation, thereby efficiently reporting on their position, but not on the fate or status of the implant. In other approaches, iodo-atoms are covalently attached to the polymer chain, for example by developing radiopaque monomers or by capping or postmodification of prepared polymers. Reported materials include, polyether-polyurethanes,[24] poly(meth)acrylates,[25–27] biodegradable polycarbonates,[28,29] polyanhydrides,[30] polyester hydrogels,[31] and poly(ester-urethane)s.[32] Aldenhoff et al. have reported that the 4-iodo benzoate CA groups that they have incorporated in their polymethacrylates are stable except when exposed to γ-irradiation.[33] None of the above polymers are both biodegradable and elastomeric (rubber-like) at 37 °C.

In our approach to develop materials for cardiovascular in situ TE applications, we have selected synthetic thermoplastic elastomers (TPEs) for detailed exploration. These materials are relatively soft and are well known to retain their shape while enduring strain and stress, which features are common to and required for most cardiovascular tissue. Because of the synthetic nature of these polymers, their properties can be tuned to meet specific requirements. For this imaging study we have chosen PCL2000-U4U as base biomaterial, a previously reported polyester with alternating polycaprolactone (PCL) soft block, and butylene bisurea (U4U) hard block segments in its macromolecular structure. It has been found that PCL2000-U4U is an elastomeric, semicrystalline, noncytotoxic and biodegradable material that can be processed by electrospinning to achieve highly porous scaffolds.[34] Furthermore, we have designed and prepared a novel CT CA that has the same butylene bisurea group in its structure: the I-U4U material (see **Figure 1** and the Supporting Information). Strong hydrogen bonding interactions between the matching U4U bisurea groups incorporate the CT CA noncovalently into the PCL2000-U4U base biomaterial, thereby creating a supramolecular and modular radiopaque biomaterial. We have adopted this modular approach from earlier work in which biomaterials with added function have been developed by combining base biomaterials with peptides, where both these components contained the supramolecularly interacting bisurea (U4U) or ureido-pyrimidinone (UPy) motif.[35–39] Note that mixing bisurea components with nonmatching supramolecular motifs has been shown to give suboptimal anchoring of the components within the modular material[34–35] (see also the Supporting Information). In a further example, we have created modular and supramolecular UPy-hydrogels that can be imaged with MRI.[40] Finally, in conjunction with and related to this work, we have closely examined the PCL2000-U4U biomaterial, particularly with regard to the characterization and mechanical testing of electrospun meshes after in vitro degradation by exposure to enzymes and oxidative species,[41,42] the in vitro macrophage action on scaffold meshes,[43] and the in vivo use of electrospun scaffolds.[44] These studies have confirmed the noncytotoxic and elastomeric character of this synthetic material.

For the present study, we have fabricated radiopaque scaffolds by electrospinning the PCL2000-U4U elastomeric biomaterial together with the newly introduced I-U4U CT CA (Figure 1). The prepared porous scaffolds have been studied by scanning electron microscopy (SEM) and differential scanning calorimetry (DSC) to investigate the scaffold morphology and

Dr. G. C. van Almen, Prof. P. Y. W. Dankers, Prof. C. V. C. Bouten
Institute for Complex Molecular Systems
Eindhoven University of Technology
Dolech 2, Eindhoven, The Netherlands
Dr. R. P. J. Budde
Department of Radiology
Erasmus Medical Center Rotterdam
's-Gravendijkwal 230, Rotterdam, The Netherlands

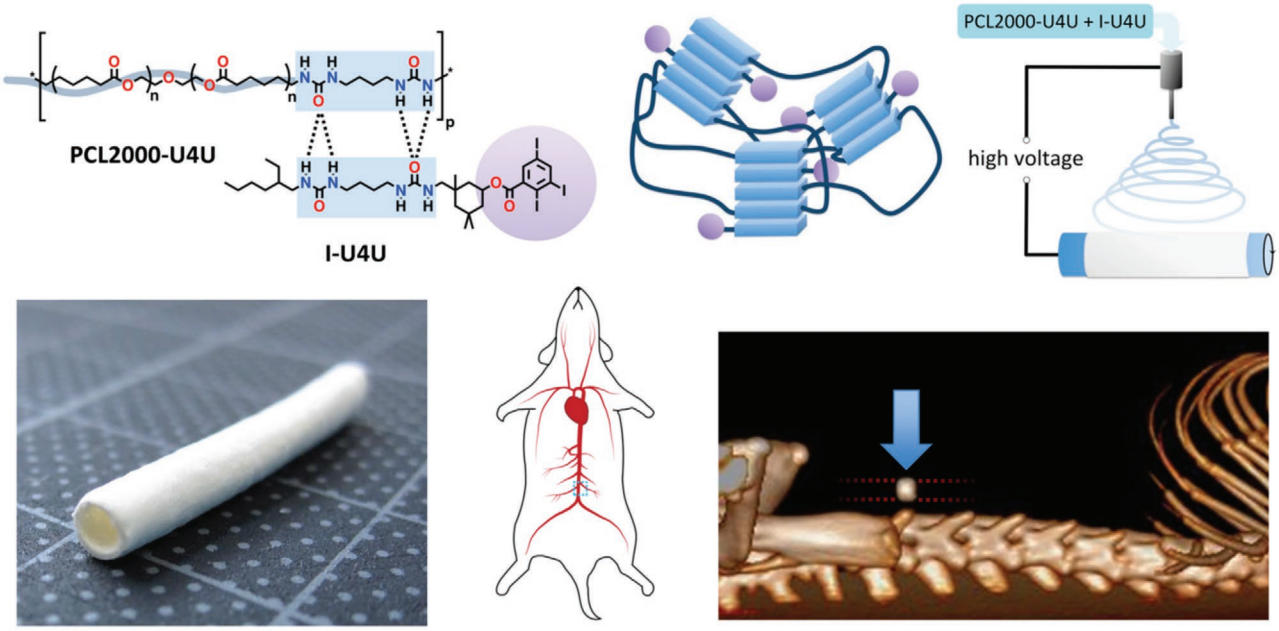

Figure 1. Schematic representation of the study. The polycaprolactone based elastomeric biomaterial PCL2000-U4U and the contrast agent I-U4U interact via supramolecular hydrogen bonding interactions between the bisurea (U4U) units (blue boxes), so that the iodinated species (purple circles) get incorporated into the modular radiopaque biomaterial. Simply mixing both components in the desired ratio in solution followed by electrospinning produces small caliber vascular grafts (photo). The in situ TE scaffolds are implanted as aortic interposition grafts in rats and are monitored in time using CT, visualizing their degradation noninvasively.

the material morphology, respectively. The scaffolds have been implanted as aortic interposition grafts in rats (n = 24), where the test group of animals received grafts composed of PCL2000-U4U and I-U4U, and the control group received grafts composed of only PCL2000-U4U (n = 12 for both groups). The animals have been sacrificed at three time points (1 day, 14 days, and 1 month; n = 4 for all time points). Degradation of the synthetic implants has been monitored noninvasively by CT scanning, while explantation of the grafts allowed the investigation of scaffold degradation by GPC. The explants of both groups were also examined by (immuno)histochemistry to study the neo-tissue formation that had taken place during the implantation period.

2. Experimental Section

2.1. The I-U4U Contrast Agent and the PCL2000-U4U Elastomer

The synthesis and characterization of the I-U4U contrast agent is fully described in the Supporting Information section. Details on the PCL2000-U4U elastomeric biomaterial and its preparation can be found along with the details on methods that were used to characterize PCL2000-U4U (Supporting Information).

2.2. Fabrication of Aortic Interposition Grafts by Electrospinning

Three types of scaffold grafts with a total iodide content of 0, 11.4, and 15.2 wt%, respectively, were prepared by electrospinning.

2.2.1. Solutions for Electrospinning

A first solution was prepared by dissolving PCL2000-U4U at a concentration of 12.5 wt% in chloroform/methanol (1 wt% methanol), while for a second solution PCL2000-U4U and I-U4U were dissolved in the same solvent mixture at a concentration of 12.5 and 4.8 wt%, respectively. A third solution was 12.5 wt% in PCL2000-U4U and 7.3 wt% in I-U4U. These weight percentages were all weight of material per weight of solution.

2.2.2. Fabrication of the Scaffold Grafts

The three solutions (see above) were sealed in a container and were magnetically stirred for 4 h at room temperature so that homogeneous dissolution of PCL2000-U4U with or without I-U4U was ensured. Next, scaffolds were fabricated by electrospinning of the polymeric solutions (using IME Technologies electrospinning equipment). The electrospun fibers were collected on a rotating cylindrical mandrel target that was 2.1 mm diameter in size to form a highly porous cylindrical object (tube). For all experiments, a flow rate of 25 µL min^{-1} was used. The solution was driven through a horizontally fixed nozzle, and toward the grounded rotating cylindrical collector that was held at a distance of 10 cm. A potential difference of 14 kV was applied between the nozzle and the target. During spinning, the temperature and humidity were kept constant at 23 °C and 30%, respectively. Finally, the prepared tubes were dismounted from the mandrel and were cut into the scaffolds that could be used for implantation. The electrospun tubes were treated with 70% ethanol by spraying and were then left to dry.

2.3. Characterization of the Electrospun Scaffolds

2.3.1. DSC

Samples of the electrospun scaffolds with iodide contents of 0, 11.4, and 15.2 wt%, as well as a neat I-U4U sample were analyzed by DSC using a TA Q-2000 machine. Melting transitions (T_m) were assessed in the first heating run (10 °C min^{-1}) and were reported by their temperature peak, while glass transitions (T_g) were recorded in the second heating run (40 °C min^{-1}).

2.3.2. SEM

An SEM (Quanta 600F) was used to observe the porous structure of the fabricated scaffolds with 0 and 11.4 wt% iodide content. SEM images were obtained before and after sterilization of the scaffolds. Prior to SEM analysis, the samples were mounted onto a holder and were sputtered with gold using a Cressington sputter coater. SEM images were taken at different magnifications using a 2 kV beam. The obtained images were analyzed with ImageJ software to assess the diameter of electrospun fibers and the wall thickness of the tubes.

2.3.3. Porosity

Multiple scaffold samples were weighed accurately, and the volumes of these electrospun scaffolds were assessed by measuring the outer diameter and the length of the scaffold by employing a digital caliper. The inner diameter of the scaffold was equal to the size of the mandrel (2.1 mm). The densities of the bulk materials were estimated by assuming a density of 1.15 g mL^{-1} for PCL2000-U4U (PCL itself has a density of 1.15 g mL^{-1}), and of 1.53 g mL^{-1} for I-U4U. This density estimation for I-U4U was based on the relative molecular weights of I-U4U (i.e., 922 Da), and of a corresponding and hypothetical molecule with one methyl and two ethyl groups instead of three iodide groups (i.e., 615 Da) that was assumed to have a similar molecular volume as that of I-U4U. Finally, the density of this hypothetical molecule was estimated at 1.02 g mL^{-1} (dicyclohexyl-urea has a density of 1.02 g mL^{-1}). Given the measured weights and volumes of the scaffolds, and the estimated densities of the materials, one can (roughly) calculate the porosities of the scaffolds.

2.3.4. Water Exposure Leakage Test

Samples of the electrospun scaffold with 15.2 wt% iodide content were immersed and incubated in water (5 mg samples in 5 mL water) at room temperature for a prolonged time. At several time points (0, 2, 4, 8, 16, 36, 72, and 170 days) a sample of material was dried and measured with ^{1}H NMR in $CDCl_3$ using dimethylformamide (DMF) as internal standard (Varian 400 MHz NMR). The samples were also analyzed by gel permeation chromatography (Varian/Polymer Laboratories PL-GPC 50, equipped with a Shodex GPC KD-804 column, using DMF with 0.1% LiBr as the eluent, operated at 50 °C). At the end of the experiment the supernatant water was examined with high performance liquid chromatography photo diode array mass spectrometry (HPLC-PDA/MS), which apparatus was a Shimadzu LC-10 AD VP series LC coupled to a PDA detector (Finnigan Surveyor PDA Plus detector, Thermo Electron corporation) and an ion-trap detector (LCQ Fleet, Thermo Scientific). Analyses were executed at 298 K using an Alltech Alltima HP C18 3 µ column using an injection volume of 2 µL, a flow rate of 0.2 mL min^{-1}, and a MeCN in H_2O gradient (from 5% to 100% MeCN, where both MeCN and H_2O contain 0.1% formic acid).

2.3.5. Cytotoxicity Test

The electrospun scaffolds (0, 11.4, and 15.2 wt%) were incubated in complete culture medium (DMEM from Gibco, supplemented with 10 v/v% fetal bovine serum (FBS) and 1 v/v% PenStrep) at 37 °C and 5% CO_2. Samples were extracted for 24 h in a weight per volume ratio of 20 mg scaffold per milliliter complete medium. 3T3 mouse fibroblasts were seeded at a density a 5×10^3 cells per well in a 96-well plate and were maintained for 24 h under standard culturing conditions until cells were grown to 50% confluence. Next, the medium was removed and 3T3 fibroblasts were cultured for an additional 24 h in the presence of 100 µL of the filtered extract. Cells exposed to complete medium supplemented with 1 v/v% Triton-X 100 served as an internal control for cytotoxic conditions. The cytotoxicity was determined using a MTT cytotoxicity assay. Briefly, thiazolyl blue tetrazolium bromide (MTT) (from Sigma) was dissolved in phosphate buffered saline to a concentration of 5 mg mL^{-1}, filtered and further diluted in complete medium to a final concentration of 1 mg mL^{-1}. The extract medium was removed and replaced with 50 µL of the MTT/culture medium. Fibroblasts were incubated for 2 h under standard culturing conditions before the MTT solution was removed and replaced with 100 µL of isopropanol (acidified with 0.04 M HCl) until all formazan crystals dissolved. Subsequently, the absorbance was measured at 570 nm (650 nm reference wavelength) on a Tecan Safire microplate reader. Cell viability was presented relative to that of 3T3 fibroblasts that were maintained in untreated culture medium during the course of the study, where this reference was set at 100% cell viability.

2.4. Implantation and Explantation of the Electrospun Scaffolds

2.4.1. Animals

The institutional Animal Care and Use Committee of the University of Utrecht, the Netherlands, approved all procedures. Twenty-four healthy male Sprague Dawley rats (300–400 g), purchased from Charles River Laboratories, were housed in groups of 3 and were fed ad libitum. The environment was maintained at room temperature for 24 h with a light–dark cycle of 12–12 h. Rats were divided in two groups, where the test group (n = 12) received an aortic interposition graft composed of PCL2000-U4U and I-U4U (iodide content 11.4 wt%), while the control group (n = 12) received an aortic interposition graft consisting of only PCL2000-U4U (iodide content 0 wt%). All 24 grafts were wrapped by a Gore-Tex shield. Grafts were explanted at day 1 (n = 8), day 14 (n = 8), and after 1 month (n = 8).

2.4.2. Preparation of the Interposition Grafts

To prevent transmural and transanastomotic ingrowth of cells, all grafts were shielded with Gore-Tex.[5] An end-to-end anastomosis was made to a 4×10 mm^2 impenetrable Gore-Tex strip (Preclude Pericardial Membrane; Gore Medical) using interrupted sutures (10-0 Ethilon, BV-4), distally and proximally of the electrospun tube. Additionally, Gore-Tex was wrapped around the electrospun tube creating an impenetrable outer layer (Figure 4).

2.4.3. Surgical Procedure

Animals were anesthetized using Isoflurane gas. A midline laparotomy was performed and the abdominal viscera were lateralized for exposure of the inferior vena cava and the abdominal aorta. After separation of the aorta from the inferior vena cava, the segment of the abdominal aorta between the renal arteries and the aortic bifurcation was occluded with microvascular clamps. After transection of the aorta the scaffold, including the Gore-tex strips, was introduced with a proximal and distal end-to-end anastomosis using interrupted sutures (10-0 Ethilon, BV-4). Pulsatile flow distally to the graft in the aorta was confirmed after removal of the vascular clamps. All scaffolds were immediately exposed to arterial hemodynamic conditions. The abdomen was closed in two layers (3-0 Vicryl FS-2). There was no heparin administration during or after surgery. Buprenorphine was given intraperitoneally as postoperative analgesic. Before rats returned to their cages, they were assessed for evidence of acute graft thrombosis or hind limb paralysis.

2.4.4. Termination and Explantation

Prior to termination, animals were anaesthetized using a KXA-mix consisting of ketamine/hydrochloride (Narketan, 100 mg mL^{-1}), xylazine (Sedamun, 20 mg mL^{-1}) and atropine (Atropine-sulfate PCH, 1 mg mL^{-1}). Rats received 0.2 mL/100 g KXA-mix intraperitoneally. An abbocath was introduced in the left jugular vein or tail vein, so that nonionic blood pool contrast agent could be administered during CT scanning. After the CT scan was made (see below), the graft was carefully explanted. Explants were fixed in 4% formalin for immunohistochemistry. Explants used for subsequent GPC analysis were treated with undiluted Clorox solution (a 5.25% aqueous sodium hypochlorite NaOCl solution) for 20 min, which was sufficient for the removal of integrated tissue. Thereafter these explants were rinsed with phosphate-buffered saline (PBS) and were left to dry for further analysis.[45]

2.4.5. GPC

The PCL2000-U4U reference material as well as recovered synthetic materials from the Clorox treated explants (≈0.5 to 1 mg amount per sample) were dissolved in 0.75 mL DMF with 0.1% LiBr. The solutions were filtered over a 0.2 µm syringe-filter and analyzed in duplicate (two separate injections) on a Varian/Polymer Laboratories PL-GPC 50 operated at 50 °C, equipped with a Shodex GPC KD-804 column, and using DMF with 0.1% LiBr as the eluent. Accordingly, the number averaged (M_n) and weight averaged (M_w) molecular weights as well as the molecular weight distributions (polydispersities $D = M_w/M_n$) relative to PEG standards were determined. Standard deviations of the M_w values for the individual animals are given (from the duplicate measurements). The averaged M_w values at every time point are also given, including the standard deviations on these averages.

2.5. CT Scanning

2.5.1. Procedure

CT acquisitions were performed on a 256-slice CT scanner, (iCT, Philips Healthcare, The Netherlands). The scan range included the entire body of the animal. Exposure parameters were 120 kV tube voltage and 500 mAs effective tube current. First, imaging was done without the use of arterial contrast agent. Subsequently, all animals were injected iodinated nonionic contrast agent at a flow rate of 0.2 mL s^{-1} (Ultravist 300 mg mL^{-1}, iopromide, Bayer Healthcare, USA) through the left jugular vein or the tail vein. The images enhanced with arterial contrast agent were used to assess graft patency. Image acquisition was started after an 8 or 15 s delay. Images were reconstructed at 0.9 mm slice thickness with a 0.45 mm increment and were transferred to a dedicated workstation.

2.5.2. Volume and Length Measurements

Using the noncontrast enhanced images, the volume and the length of the PCL2000-U4U with I-U4U grafts were calculated. First 3D volume rendered images were generated using a custom image filter that included all voxels with a Hounsfield unit (HU) value higher than 175 HU. Using electronic tools, the graft was digitally excised and its volume measured.

2.5.3. Density Measurements

On standard noncontrast enhanced axial images, a circular region of interest (ROI) following the outer boundary of the graft was placed on the graft at three levels in its proximal, middle, and distal part. The mean signal intensity and standard deviation of signal intensities in the ROI were measured.

2.6. Histology

2.6.1. Immunohistochemistry

Explants were fixed in formalin 4% before preembedding in 1% agar (Eurogentec), followed by embedding in paraffin. Consecutive 4 µm sections were stained with hematoxylin and eosin (HE) for basic morphology and with PicroSirius red (PSR) for

detection of collagen. Immunohistochemical stains to detect macrophages were performed after antigen retrieval in citrate buffer using a monoclonal mouse anti-CD68 antibody (Serotec, MCA341GA, 1:400).

2.6.2. Quantitative Histologic and Immunohistological Analysis

Two investigators, who were blinded to the investigated groups and the time point of explantation, independently conducted the analyses. Sections were photographed using a Nikon E800 microscope with ACT-1 software. For the measurement of the mean wall thickness and the mean lumen diameter, each slide was studied under a 2× objective lens. The cellularity was studied under high-power magnification (high-power field (hpf), 40× objective lens; area comprising 0.034 mm^2). The total number of cells in four random hpf areas per PCL2000-U4U tube (with or without I-U4U) was manually counted using ImageJ software.

Quantification of collagen content was performed with PSR stains and circularly polarized light. Per stained section, four random hpf fields were digitally photographed, and areas positive for collagen were marked and binarized. The positive areas were measured as a percentage of the total surface. A quantitative analysis of the immunopositive cells (CD68) of each stained slide was performed at four random hpf fields. The area of positive cells was measured within four hpf images as a percentage of the total from binarized images. The mean for four high power images was then calculated for each sample.

2.7. Statistical Analysis

Numerical data are presented as the mean ± standard deviation. Statistical differences were determined using a student's *t*-test or a Mann–Whitney test for nonparametric data, using Prism (GraphPad Software). Kruskal–Wallis test was used to measure statistical differences in scaffold density. $p < 0.05$ was considered statistically significant. Linear regression analysis was performed to compare slopes.

3. Results and Discussion

3.1. Synthesis of the I-U4U Contrast Agent and Material Characterization

The I-U4U bisurea CA was synthesized starting with the reaction of racemic 2-ethyl-1-hexylamine with butane diisocyanate to prepare the mono-urea intermediate **1**, that was isolated as an oil (**Scheme 1**). The activated building block **2** was prepared from 2,3,5-triiodo-benzoic acid in two steps according to a reported procedure.[46] The cyclic and branched aminol **3**, that is in fact a mixture of isomers, was amine protected with

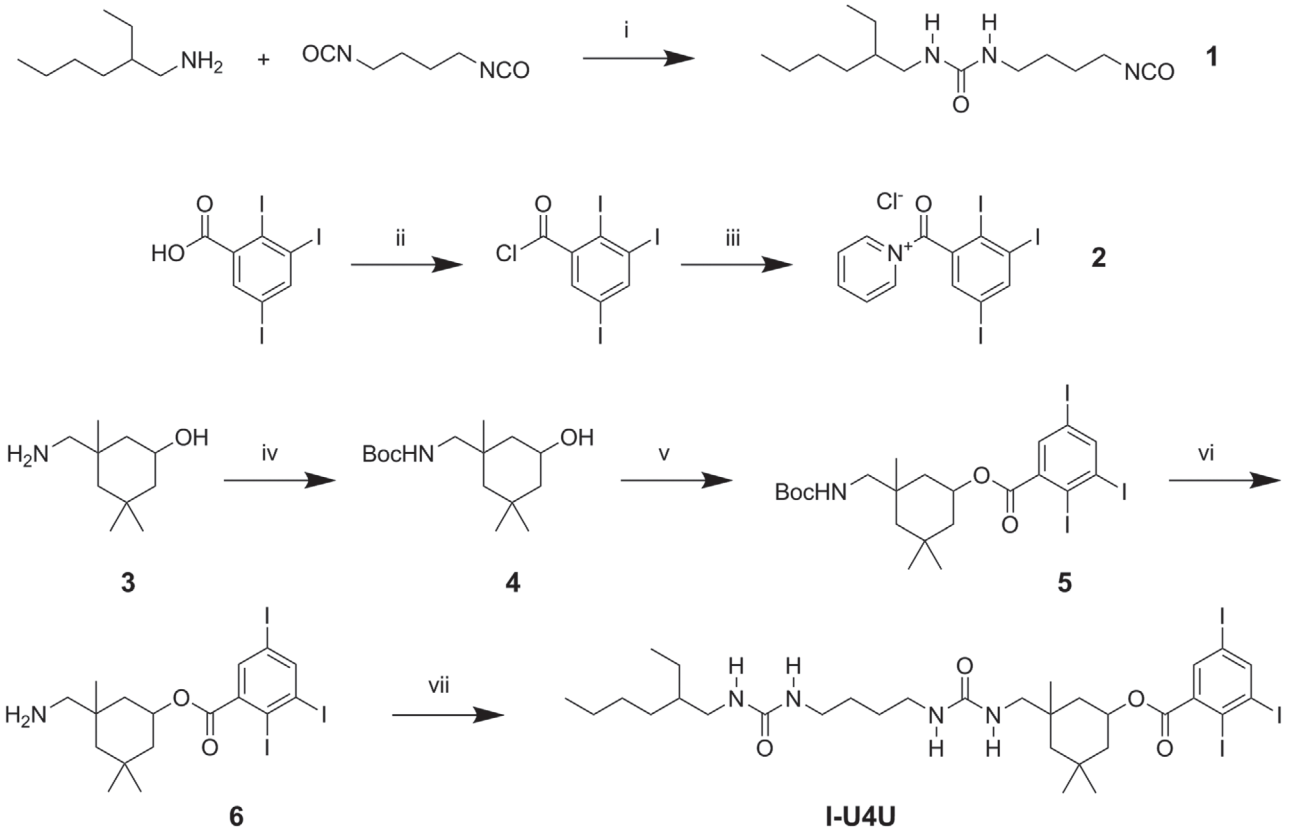

Scheme 1. Synthesis of contrast agent I-U4U. Reagents and solvents: i) chloroform, acetonitrile; ii) oxalylchloride, DMF, dichloromethane; iii) chloroform, pyridine; iv) di-*tert*-butyl dicarbonate, DIPEA, isopropanol; v) **2**, dichloromethane; vi) TFA, dichloromethane; vii) **1**, DIPEA, dichloromethane.

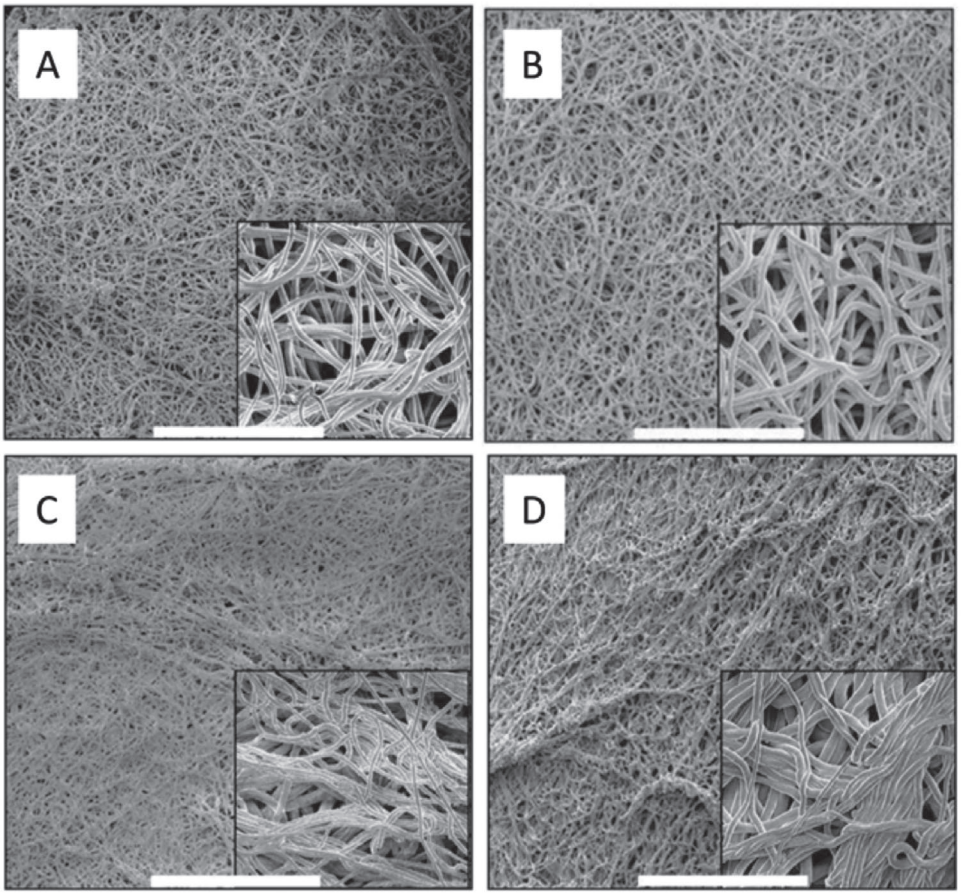

Figure 2. SEM images of scaffolds electrospun from chloroform/methanol (1 wt% methanol). All pictures show the outer surfaces of the scaffold tubes. A,B) Reference PCL2000-U4U grafts without iodide and C,D) iodinated PCL2000-U4U/I-U4U grafts with 11.4 wt% iodide, A,C) before and B,D) after sterilization with ethanol/water. The full lengths of the white bars represent 400 μm (for overviews) and 100 μm (for insets), respectively.

a Boc-group and was thereafter connected to the benzoyl pyridinium chloride **2** to prepare the ester building block **5**, which intermediate was isolated in a 65% yield after column chromatography. Deprotection of the Boc group using TFA in dichloromethane gave the TFA-salt product of **6**, that was coupled to isocyanate **1** to arrive at the CT-CA end product I-U4U. After purification I-U4U was isolated in a 35% yield. I-U4U was well-soluble in organic solvents such as for example chloroform.

The PCL2000-U4U material base material was prepared successfully, with NMR data matching those from literature,[34] and with recorded molecular weights being sufficiently high (M_w = 63.4 kDa, M_n = 31.7 kDa; D = 2.0). The bulk material showed similar mechanical properties to those reported, as tensile tests on cast films gave a Young's modulus of E = 15.9 ± 0.4 MPa, a strength at break (and UTS) of σ-break = 27 ± 3 MPa, a strain at break of ε-break = 1001 ± 98% and a tensile toughness of U_T = 154 ± 21 MPa.

3.2. Preparation and Characterization of the Electrospun Scaffolds

Radiopaque vascular grafts were prepared by incorporating contrast agent I-U4U into the PCL2000-U4U biomaterial, simply by mixing these two components in solution with subsequent electrospinning. Reference PCL2000-U4U grafts without I-U4U were also prepared. Grafts with inner diameters that match those of native aortas of rats were prepared (2.1 mm). The scaffold materials were designed and fabricated to contain 0, 27.7, and 36.9 wt% I-U4U, respectively, corresponding to scaffold grafts with 0, 11.4, and 15.2 wt% iodide contents, respectively. Molar ratios between the bisurea groups of I-U4U and PCL2000-U4U in the two modular biomaterials thus were ≈1:1 and ≈8:5, respectively.

The wall thickness of the scaffolds was in the 0.3 ± 0.1 mm range, as determined by SEM. The fiber structure and the orientation in the electrospun scaffolds was also studied using SEM. **Figure 2** shows the outer surfaces of the scaffolds. The scaffolds were porous, with the PCL2000-U4U reference material showing a more homogeneous structure of fibers and open spaces, with clustered fibers being less abundant than in the iodinated PCL2000-U4U/I-U4U material. For both the reference and the iodinated scaffolds, fibers on the inner surfaces of the grafts showed a more flattened appearance (not pictured) as compared to the fibers seen at the outer surfaces. The mean fiber diameter in the reference PCL2000-U4U scaffolds was 4.5 ± 0.5 μm, while the electrospun PCL2000-U4U grafts containing 11.4% iodide showed fiber diameters of 4 ± 1 μm

Table 1. Compiled electrospinning conditions and results.

Scaffold	Conditions			Results		
	Conc.[a] [wt%]	Voltage [kV]	I.d.[b] [mm]	Wall thickness [mm]	Porosity [%]	Fiber thickness [µm]
PCL2000-U4U	12.5	14	2.1	0.3 ± 0.1	65	4.5 ± 0.5
PCL2000-U4U + I-U4U	12.5 + 4.8	14	2.1	0.3 ± 0.1	62	4 ± 1

[a]From chloroform with 1 wt% methanol; [b]Inner diameter of graft, diameter of mandrel.

(**Table 1**). Sterilization did not influence the overall structure. The calculated porosities of the scaffolds with 0, 11.4, and 15.2 wt% iodide contents were about 65%, 62%, and 66%, respectively.

Thermal analysis using DSC was performed to investigate the morphology of the modular materials. The reference PCL2000-U4U scaffold showed a weak and broad melting transition at 54 °C (ΔH = 1.2 J g^{-1}) for the crystalline PCL domains, and another broad melting transition at 119 °C (ΔH = 11.6 J g^{-1}) for the melting of the U4U bisurea aggregates. A glass transition at −56 °C was recorded for the amorphous phase of this material. The PCL2000-U4U/I-U4U iodinated biomaterial scaffolds with 11.4 and 15.2 wt% iodide displayed broad and weak melts at 54 °C (ΔH = 1.0 J g^{-1}) and 56 °C (ΔH = 1.4 J g^{-1}), respectively, melting transitions for the U4U stacks at lowered temperatures of 104 °C (ΔH = 9.1 J g^{-1}) and 105 °C (ΔH = 6.5 J g^{-1}), respectively, and T_g at −56 and −57 °C, respectively. The neat and solid I-U4U contrast agent itself showed a weak and broad melting transition at 53 °C (ΔH = 4.0 J g^{-1}).

Incubation in water of the selected radiopaque scaffold with the highest amount of iodide (15.2 wt% content), at room temperature and over a period of 170 days, did not change the composition of the material as assessed by ^{1}H NMR analysis on dried scaffold samples. The molecular weight of the PCL2000-U4U material also remained constant over the 170 day testing period. The water that was exposed to the iodinated scaffold remained clear over time and did not contain any solutes that could be traced back to PCL2000-U4U or I-U4U, as assessed by HPLC-PDA/MS.

None of the investigated scaffold grafts showed cytotoxic effects, indicated by the MTT-assay using 3T3 fibroblasts (**Figure 3**). Particularly, addition of I-U4U, either 11.4 or 15.2 wt%, did not cause an adverse effect on the observed cell viability.

3.3. Implantation and CT Scanning

The iodinated scaffolds with the lowest iodide content of 11.4 wt% were selected for implantations (**Figure 4**). Of the 24 animals, 2 animals did not survive due to intraoperative bleeding near the Goretex-electrospun tube anastomosis. The mean operation time was 1 h and 26 min with a mean vascular clamp time of 39 min. Postoperative complications did not occur for the 22 surviving animals, with no signs of infections or hind limb paralysis.

The iodinated grafts with 11.4 wt% iodide were clearly visible on CT images. At day 1, a high-density signal was seen (**Figure 5**A,D,E). Grafts had a mean length of 6.4 mm, and a mean diameter of 3.6 mm. The Goretex at the proximal and distal side of the electrospun tube and the Goretex wrapped around the whole graft could not be assessed on the CT images. Because of the similar radiopacity of PCL2000-U4U and soft tissue, the control grafts without iodide were not visible on CT images (Figure 5B), only its lumen could be evaluated on contrast enhanced scans (Figure 5C). All grafts were patent (Figure 5C,E).

Axial CT images as recorded in time clearly showed that the contrast disappeared (**Figure 6**A–C), especially when comparing the image at day 1 with that at day 30. Coronal CT images confirm this observation (Supporting Information). The measured CT contrast volume of the implanted grafts decreased significantly in time (Figure 6D), as before implantation the iodinated grafts had a volume of 6.01 mm^3, while at day 30 a volume of 2.56 mm^3 ± 1.67 mm^3 was recorded (p = 0.035). Intermediate points seemed to display a decrease in average value (5.16 mm^3 ± 1.9 mm^3 at 1 day, and 4.3 mm^3 ± 1.1 mm^3 at day 14), The CT contrast density of the scaffold was quantified by measuring HU on axial images (Figure 6E), and over time an inhomogeneous decrease of this density was observed. The mean density at day 30 was significantly lower when compared to those at day

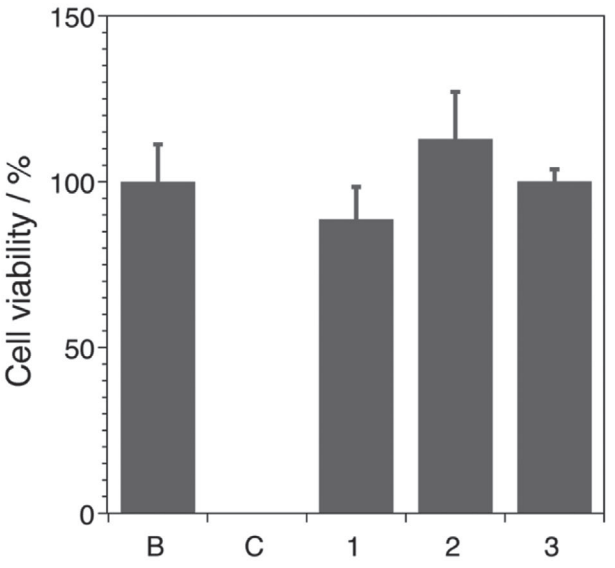

Figure 3. Cell viabilities as determined using an MTT assay, where 3T3 fibroblasts have been exposed to complete culture medium after it had been incubated with electrospun meshes of 1) PCL2000-U4U, 2) PCL2000-U4U/I-U4U (11.4 wt%), and 3) PCL2000-U4U/I-U4U (15.2 wt%). The cell viability is presented relative to the cell survival observed for fibroblasts that were maintained in untreated medium (reference blank B), and that was set at 100%. Exposure to Triton-X 100 surfactant has been used as a further control (C).

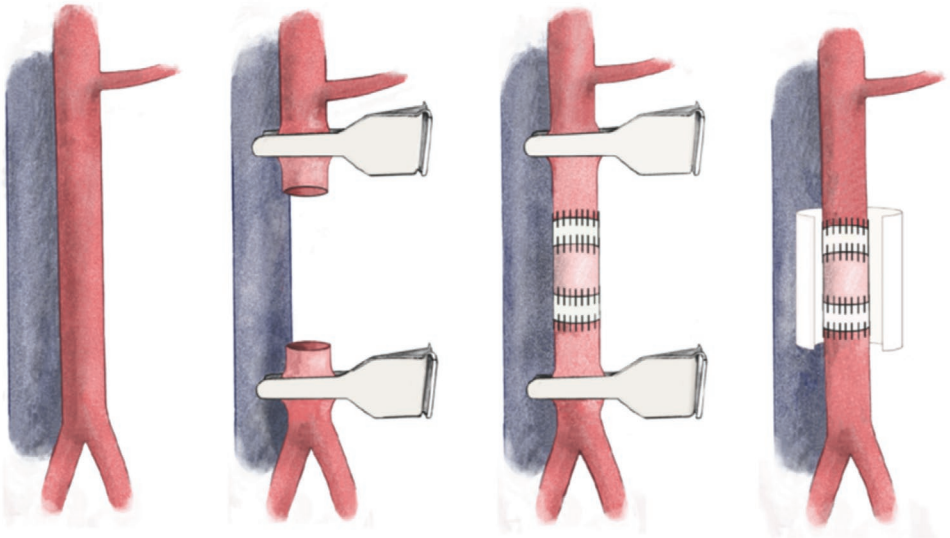

Figure 4. Schematic representation of the surgical procedure. From left to right: the abdominal aorta (red) is prepared free from the inferior vena cava (blue); after occlusion with vascular clamps the abdominal aorta is transected; implantation of the interposition graft composed of impenetrable GoreTex and electrospun PCL2000-U4U with or without I-U4U; removal of the vascular clamps, and wrapping of a GoreTex sheet around the graft. This animal model has been developed to induce ingrowth of circulating cells from the blood stream only, thereby mimicking the human situation.[5,57]

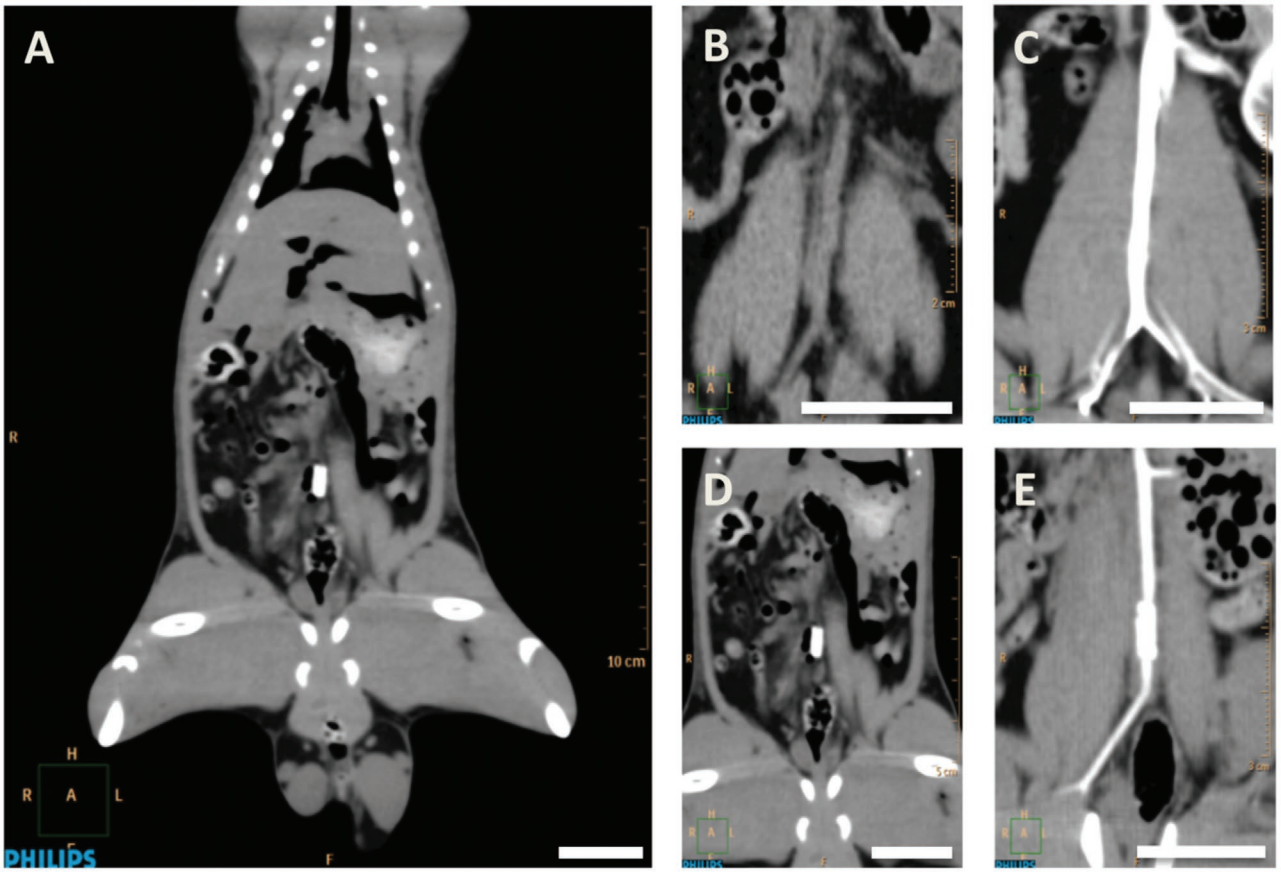

Figure 5. CT images of the aortic interposition grafts in rats, 1 day after implantation. A) Overview; aortic interposition graft composed of PCL2000-U4U and I-U4U (11.4 wt% iodide). B,C) Control PCL2000-U4U graft and D,E) test PCL2000-U4U/I-U4U graft, B,D) before and C,E) after administration of arterial CT contrast agent (iopromide, "Ultravist"). Bars indicate 2 cm.

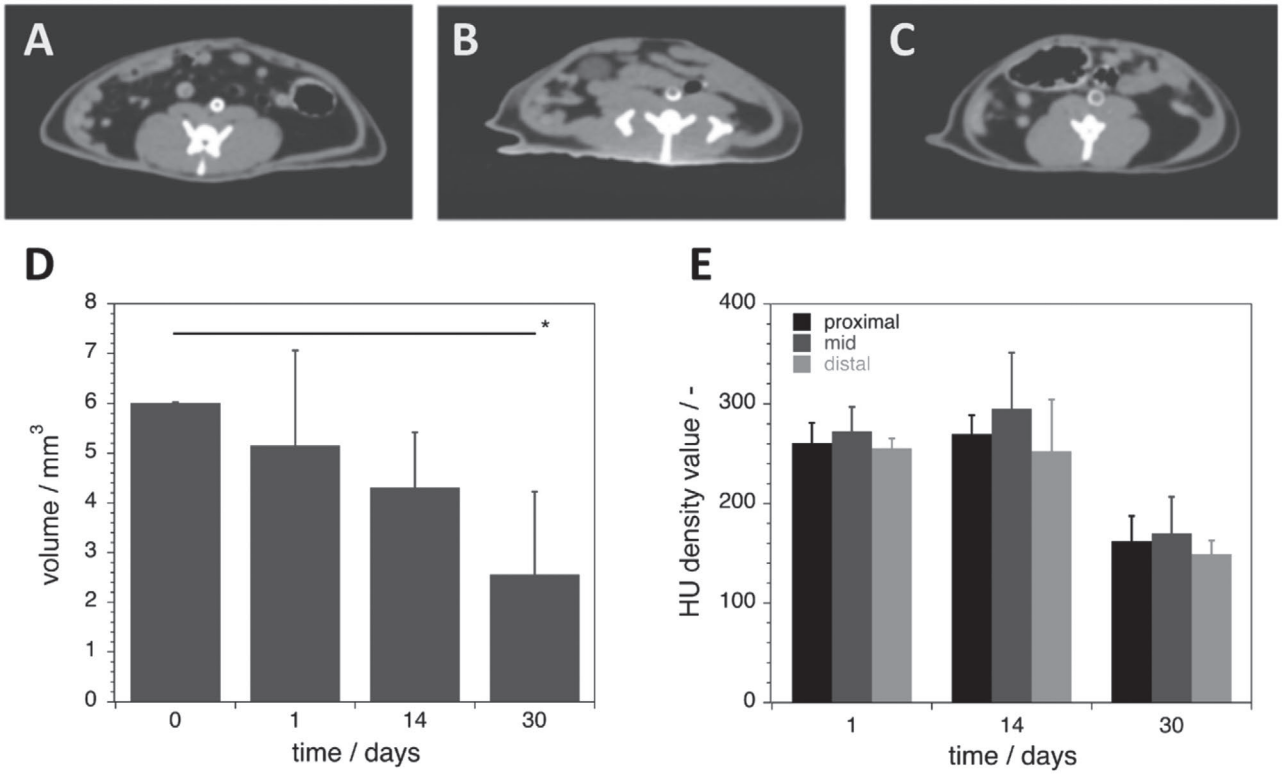

Figure 6. CT images, volumes and densities of implanted aortic interposition grafts over time. Axial images at t = A) 1 day, B) 14 days, and C) 30 days post implantation. D) Volumes measured on CT images showing a significant decrease after 30 days ($p = 0.035$) relative to $t = 0$. E) Densities as measured on axial images, at $t = 1$ day, $t = 14$ days and $t = 30$ days, and at proximal (P), mid (M), and distal (D) sections in the graft. The wider standard deviations seen at day 14 after implantation indicate more inhomogeneous densities.

1 ($p < 0.001$) and day 14 ($p < 0.001$). Furthermore, standard deviations increased with the largest deviations seen at $t = 14$ days.

3.4. Implant Degradation Analysis

The PCL2000-U4U material recovered from explants was analyzed by GPC to record its molecular weight (**Table 2**), to thereby assess if PCL2000-U4U had degraded while being implanted. In multiple cases, and especially for explants that had been implanted for 30 days, the synthetic implant material had degraded completely as no material could be traced. In these cases, obviously, no GPC analyses could be conducted. After 1 day, eight out of eight explant samples gave recovered material that could be analyzed, while after 14 days five out of six explant samples, and after 30 days, (only) three out of eight explants gave some recovered synthetic material for analysis. Derived from the limited available molecular weight data in Table 2, it seems that the PCL2000-U4U material lowers in molecular weight in time.

3.5. (Immuno)Histochemical Analysis

The explanted grafts showed no stenosis or thrombosis (**Figure 7**, HE staining). One month after implantation grafts had dilated. The mean diameter increased over time with 2.09 ± 0.09 mm and 2.20 ± 0.46 mm at day 1, 2.56 ± 0.12 mm and 2.33 ± 0.47 mm at day 14 and 2.81 ± 0.62 mm and 2.88 ± 0.25 mm at day 30, for the implants in the I-U4U test group and the non I-U4U control group, respectively. The wall thickness of the implanted

Table 2. Weight averaged molecular weights (M_w) as determined by GPC analysis of PCL2000-U4U material as recovered from explants. Values are in kDa. Dispersities D (M_w/M_n) gave little deviation with values between 1.8 and 2.4 for all samples (data not shown). It is indicated when no material (n.m.) for GPC analyses was recovered, when the animal had died (–), and when 1 instead of 2 GPC measurements were performed due to too little material being recovered (*). Day 0 represents the M_w of PCL2000-U4U prior to implantation.

M_w data from GPC	Day 0	Day 1	Day 14	Day 30
Test group with I-U4U		54.8 ± 0.0	53.4 ± 0.3	51.3 ± 0.8
		53.1 ± 0.4	48.1 ± 1.3	27.6 ± 0.7
		54.6 ± 0.6	–	n.m.
		51.1 ± 0.1	38.8 ± 4.2	n.m.
Average	59.3 ± 0	53.4 ± 1.7	46.8 ± 7.4	39.4 ± 16.7
Control group without I-U4U		49.0 ± 0.1	n.m.	44.7*
		59.3 ± 0.5	–	n.m.
		47.4 ± 0.4	50.2 ± 0.6	n.m.
		48.3 ± 0.4	65.5 ± 1.8	n.m.
Average	63.4 ± 0.3	51.0 ± 5.6	57.8 ± 10.8	44.7

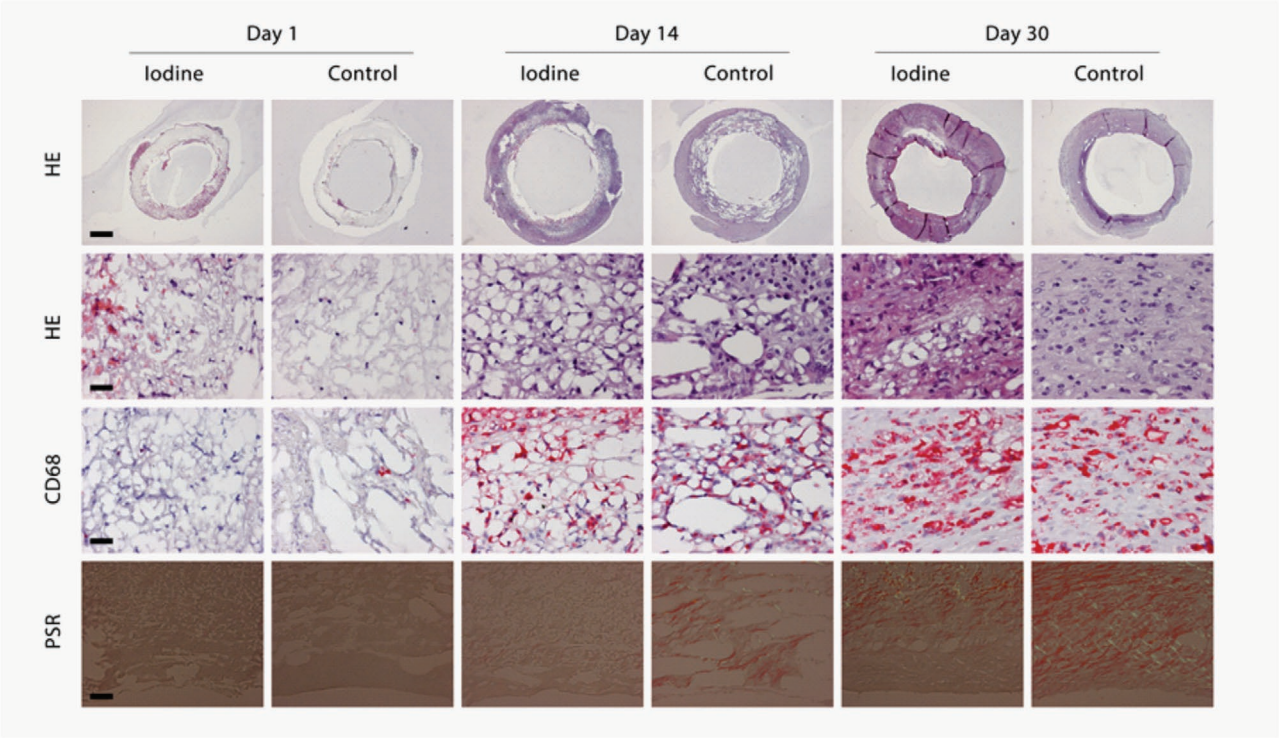

Figure 7. Histology of explanted iodinated and control grafts at day 1, 14, and 30. Applied are HE staining, CD68 for macrophages and PSR for collagen. Black bars indicate 300 µm (first row HE), 20 µm (second row HE and CD68), and 50 µm (PSR). The Supporting Information provides these pictures in enlarged format.

scaffolds did not change over time. At day 1, wall thicknesses of 0.29 mm ± 0.03 mm and 0.27 ± 0.03 mm were seen in the test group and in the control group, respectively. At day 14, thicknesses of 0.21 ± 0.06 mm were observed in the test group and of 0.26 ± 0.07 mm in the control group. Finally, after 30 days a wall thickness was measured of 0.22 ± 0.04 mm in the test group and of 0.21 ± 0.05 mm in the control group. According to the above, dimensions of the implants altered in the same fashion for both groups over time. Furthermore, in the control group and the test group, cells penetrated and spread immediately after implantation into and over the entire thickness of the graft. At day 1 a limited number of cells had infiltrated the graft (10 ± 12 cells per hpf in the test group and 2 ± 1 cells per hpf in the control group) (Figure 7, HE staining second row; **Figure 8**A). This number increased to 60 ± 12 cells per hpf at day 14, and 90 ± 20 cells per hpf at day 30 in the test group. In the control group this number increased to 93 ± 19 cells per hpf at day 14, and 113 ± 22 cells per hpf at day 30. Over 30 days the number of cells increased significantly in both the test group ($p = 0.03$) and the control group ($p = 0.03$). The number of cells in the test group compared to that in the control group seemed somewhat lower at the 14 day time point, but in fact did not significantly differ at each time point (Figure 8A).

At day 1 cellular infiltrate consisted mainly of neutrophilic granulocytes. In a second healing phase CD68 positive cells (macrophages) infiltrated the graft (Figure 7, CD68 staining; Figure 8B). At day 1 a positive area fraction was seen of 0.03% ± 0.03% in the test group compared to 0.17% ± 0.02% in the control group. At day 14 an area fraction of 1.51% ± 0.57% in the test group compared to 0.88% ± 0.63% in the control group was seen. This area increased further to 2.76% ± 1.41% and 2.02% ± 0.75% at day 30 in, the test and the control group, respectively. A significant increase in CD68 positive cells was seen from day 1 to day 30 in both the test group and the control group ($p = 0.02$ for both groups). The area fraction did not differ significantly for the test group as compared to the control group at all time points (Figure 8B). The collagen surface produced by day 30 was similar in both groups with an area fraction of 1.26% ± 1.03% in the test group compared to 1.15% ± 0.63% in the control group ($p = 0.85$) (Figure 7, PSR staining; Figure 8C).

The histology data attest that the implanted synthetic material degrades in vivo in time. Particularly, the histology pictures show heterogeneously sized white areas in all panels (Figure 7, HE and CD68 stainings). These white areas indicate synthetic material,[5] in this case PCL2000-U4U with or without added I-U4U CA. Clearly, the white areas are smaller and far less abundant in the explants after 30 days of implantation than in the other explants.

3.6. Discussion

We have developed a new CT-imaging contrast agent I-U4U that has a 41 wt% iodide content and that can be used for monitoring the degradation of cardiovascular substitutes used in in situ tissue engineering. I-U4U is decorated with an ester moiety to increase its possibilities for in vivo degradation and has

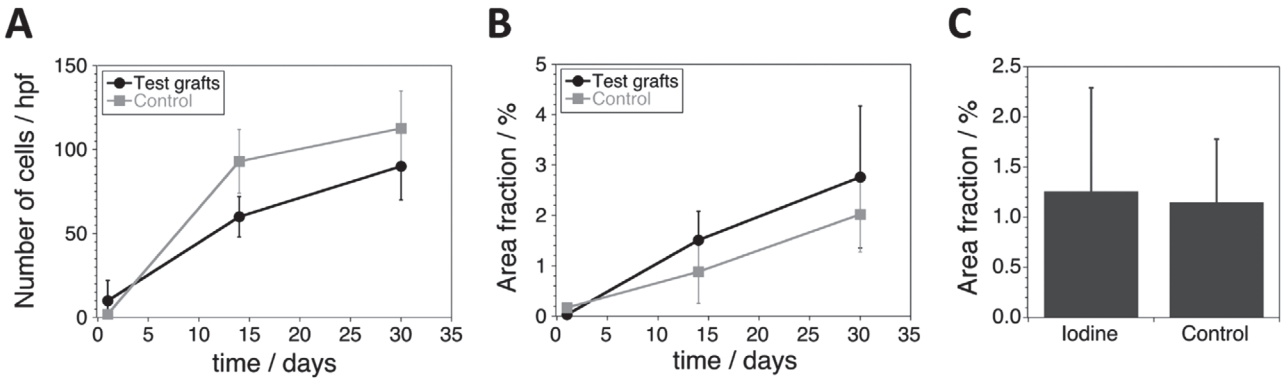

Figure 8. Comparative histology results from the explanted iodinated test grafts and the control grafts without CA. A) Cellularity at different time points as measured per hpf. B) Area fraction CD68 positive cells as a function of time. C) Matrix formation as quantified with collagen measurements after 30 days.

branching groups on either side of the U4U bisurea moiety to make it well-soluble in organic solvents, enabling its processing from solution, notably for electrospinning purposes. I-U4U can simply be mixed and processed with PCL2000-U4U to create a supramolecular and modular radiopaque biomaterial. The PCL2000-U4U component is an elastomeric and tough material (E = 16 MPa; U_T = 154 MPa; ε-break = 1000% for bulk material), which type of soft materials can be considered for cardiovascular TE as alternative to frequently applied hard, brittle and nonelastic polyester materials such as PCL, PGA, or PLA. For example and comparison, electrospun PCL is often used in TE,[47] and as a bulk material it shows an E-modulus of 250 to 450 MPa [48] and an ε-break of ≈80%.[49] These high moduli do not correspond well with those of blood vessel tissues of various mammals, including humans, as these E-moduli are in the range of 0.1 to 5 MPa.[50] Strains endured by human arteries are typically 10% to 15%.[51] Given these data, electrospun PCL2000-U4U meshes show agreeably matching E-moduli of 0.5 to 2 MPa at 5% to 15% strains.[42]

Examining the morphology of the modular PCL2000-U4U/I-U4U materials using DSC has shown that the two components are intimately mixed in the U4U hard phase of the segmented thermoplastic elastomer (TPE) material. This can be derived from the observation that the melting transition of the U4U stacks in the hard phase changes from 119 °C for PCL2000-U4U to 105 °C for PCL2000-U4U with added I-U4U. Apparently, the U4U units of both components interact with each other and together form a heterogeneous U4U hard phase. In contrast, the T_g does not change upon I-U4U addition, as it remains at ≈–56 °C, indicating that the I-U4U material does not mix into the PCL amorphous soft phase. Similar findings have been reported in a morphology study on comparable modular TPE materials based on PCL1250-U4U and a supramolecular filler component with 2-ethylhexyl groups flanking not one but both U4U urea groups.[36] For these modular materials, the U4U hard phase was shown to consist of nanofibers ≈5 nm in diameter, indicating mixing of U4U-groups along these fibers. This study also showed that U4U-filler contents as high as 60 mol% gave modular materials with somewhat higher E-moduli, but with, importantly, retained elastomeric properties.

We have selected the PCL2000-U4U/I-U4U scaffolds with the lowest investigated iodide content of 11.4 wt% for the in vivo imaging and implantation studies. First, because it has been assessed that radiopacity in bulk materials is sufficient at iodide contents of at least 3–5 wt%,[33] and given the porosities of the prepared electrospun scaffolds (≈60–65%), the 11.4 wt% scaffolds should be suitable with contents of ≈4.0 to 4.6 w/v%. Second, preliminary CT imaging tests showed that scaffolds with the iodide content of 11.4 wt% were indeed clearly visible.

The addition of I-U4U to PCL2000-U4U did not influence the cytotoxicity of the electrospun material nor did it seem to alter the cellular behavior within matrices of the material. Our results demonstrate that electrospun grafts of the test group (PCL2000-U4U with added I-U4U) and the control group (only PCL2000-U4U) are noncytotoxic to fibroblasts, and in vivo give similar trends in cellular adherence, infiltration and differentiation. Data are most comparable when considering the complete 30 days period of the implantation experiment, while some deviations (albeit not significant) were seen after 14 days. Also, the collagen production in these electrospun matrices is comparable. In both test and control group the number of cells and the amount of collagen increased over time. Gross morphology seen on HE stained slides showed initial adherence of neutrophilic granulocytes, followed by an influx of macrophages (confirmed with CD68 staining). In time, more myofibroblasts were seen which subsequently resulted in production of collagen after one month, which was confirmed with PSR staining. These results are comparable to other histological findings in in situ TE studies where colonization and subsequent remodeling of a biodegradable synthetic graft into neo-arteries has been investigated.[52–55] For our vascular implants, no differences in the measured wall thicknesses of the grafts of the test group and control group were observed. A trend toward an increase in graft diameter was monitored for both groups, implying that the grafts had not retained their original shape, and had dilated.

The in vivo scaffold degradation could be imaged and monitored noninvasively with CT scanning for the PCL2000-U4U/I-U4U test group. Both the imaging volume and density decreased significantly from day 1 to 30, while the density changed from a homogeneous to an inhomogeneous signal. Consequently, I-U4U material disappeared from the implantation site and eroded and/or degraded over the 30-day period. However, the ultimate fate of the I-U4U material was not specifically investigated in this study. Obviously, the reference

PCL2000-U4U grafts were not seen by CT-imaging, and CT-imaging of the modular PCL2000-U4U/I-U4U implants only registered material that contained iodine atoms. Therefore, scaffold degradation was also assessed by examining recovered synthetic material from explant samples. Here, it was observed that after 1 day of implantation, all explant samples contained synthetic PCL2000-U4U material for GPC analysis, while after 30 days of implantation no synthetic scaffold material was traced for the majority of the explants. Furthermore, GPC showed a loss in molecular weight for PCL2000-U4U, and histology analyses showed less abundant and smaller synthetic implant fragments over time. These scaffold degradation results qualitatively correspond with the observed decrease in CT imaging signal in time: the loss in CT-contrast coincides with a loss of PCL2000-U4U material in the explants. Apparently, I-U4U and PCL2000-U4U co-degrade and/or co-erode (see also the Supporting Information). To demonstrate a precise quantitative correlation between scaffold volume and density on CT images on one hand and scaffold degradation on the other, however, and to thereby investigate if PCL2000-U4U and I-U4U erode and degrade at (exactly) the same rate, studies involving more animals or studies involving larger grafts using larger animal models should be performed.

This study shows that the degradation of PCL2000-U4U as a porous vascular graft, i.e., in the constant presence of blood and with the constant action of strains, occurs fast and within the time frame of about 1 month. In contrast, when PCL2000-U4U was investigated as subcutaneous implants in rats, the material remained present for a longer time, up to at least the last investigated time point (42 days), albeit that the implant was a solid thin film (400 μm) and not a porous film.[34] When using porous structures for cardiovascular in vivo TE, it is presumably better to use materials that are degrading more slowly than PCL2000-U4U, allowing more time for neo-tissue to form and mature. In a study on heart valve TE we have therefore used PC-BU, a sequence controlled material similar to PCL2000-U4U, albeit with polyhexylcarbonate instead of PCL-ester soft blocks.[56]

Finally, note that our results have been obtained using an animal model that only allows infiltration of cells into the porous implant from the blood stream, so as to mimic the situation in humans.[57] Goretex sheets have been employed for this purpose. Presumably, Goretex will not be applicable in clinical settings.

4. Conclusion

Our results demonstrate that electrospun and implanted PCL2000-U4U vascular grafts with modularly added I-U4U contrast agent are clearly visible on CT images. Volume and density of the grafts can be measured and monitored conveniently. A decrease in CT signal was observed in concord with scaffold degradation. In a more general sense, this study shows that innovative biodegradable radiopaque materials can be designed and prepared by modularly combining base biomaterials with CT contrast agents, with both these components containing strongly interacting supramolecularly matching motifs, such as, e.g., U4U groups. The supramolecular interactions result in biomaterials with intimately mixed and properly anchored components that in vivo can co-erode and co-degrade. Consequently, imaging will not merely report on the CA only, but on the degrading implant as a whole. Accordingly, this supramolecular and modular approach can be applied to develop alternative, and possibly improved, radiopaque (bio)materials as compared to the solid implant materials that are currently used in CT imaging, such as material/metal or material/salt mixtures (that are usually inhomogeneous and/or nonbiodegradable), or materials that are obtained by postmodification or capping procedures (that usually have less controlled molecular structures and/or have sacrificed material properties). Taken together, the presented concept of creating solid radiopaque biomaterials in a modular and supramolecular fashion can be used to noninvasively monitor and image the biodegradation of synthetic implants.

Supporting Information

Supporting Information is available from the Wiley Online Library or from the author.

Acknowledgements

This research formed part of the iValve project of the research program of the BioMedical Materials institute, co-founded by the Dutch Ministry of Economic Affairs, Agriculture and Innovation. The financial contribution of the Nederlandse Hartstichting is most gratefully acknowledged. All members of the iValve project are thanked for valuable discussions. Joost L.J. van Dongen, Xianwen Lou (from the Macromolecular and Organic Chemistry group at the TU/e Eindhoven, the Netherlands) and Michel Fransen (SyMO-Chem BV) are thanked for their contributions and help on MS (HRMS, MALDI-TOF-MS, HPLC-MS and GC-MS) and GPC measurements.

Conflict of Interest

The authors declare no conflict of interest.

Author Contributions

H.M.J. and J.K. contributed equally to this work. H.T., L.A.v.H., A.V., R.P.J.B., J.K. were involved in imaging experiments and radiology, animal experiments, and histological evaluation. S.H.M.S., A.M.A.B., and H.M.J. designed, S.H.M.S. synthesized, and S.H.M.S. and G.C.v.A. characterized the materials. A.M.A.B. did initial imaging experiments. S.H.T. produced and characterized the electrospun implants. P.Y.W.D. and C.V.C.B. provided valuable insights regarding the project design and discussed the results. H.T. and H.M.J. wrote the manuscript.

Keywords

aortic interposition graft implants, computed tomography imaging, degrading supramolecular biomaterials, modular contrast agents, tissue engineering

Received: January 20, 2020
Revised: April 6, 2020
Published online:

[1] C. V. C. Bouten, A. Driessen-Mol, F. P. T. Baaijens, *Expert Rev. Med. Devices* **2012**, *9*, 453.
[2] A. Y. Lee, N. Mahler, C. Best, Y.-U. Lee, C. K. Breuer, *Transl. Res.* **2014**, *163*, 321.
[3] R. Langer, J. Vacanti, *Science* **1993**, *260*, 920.
[4] P. Dohmen, F. Costa, S. Lopes, S. Yoshi, F. Souza, R. Vilani, M. B. Costa, W. Konertz, *Heart Surg. Forum* **2005**, *8*, E100.
[5] H. Talacua, A. I. P. M. Smits, D. E. P. Muylaert, J. W. Van Rijswijk, A. Vink, M. C. Verhaar, A. Driessen-Mol, L. A. van Herwerden, C. V. C. Bouten, J. Kluin, F. P. T. Baaijens, *Tissue Eng., Part A* **2015**, *21*, 2583.
[6] D. E. P. Muylaert, G. C. van Almen, H. Talacua, J. O. Fledderus, J. Kluin, S. I. S. Hendrikse, J. L. J. van Dongen, E. Sijbesma, A. W. Bosman, T. Mes, S. H. Thakkar, A. I. P. M. Smits, C. V. C. Bouten, P. Y. W. Dankers, M. C. Verhaar, *Biomaterials* **2016**, *76*, 187.
[7] C. V. C. Bouten, P. Y. W. Dankers, A. Driessen-Mol, S. Pedron, A. M. A. Brizard, F. B. T. Baaijens, *Adv. Drug Delivery Rev.* **2011**, *63*, 221.
[8] J. P. Vacanti, M. A. Morse, W. M. Saltzman, A. J. Domb, A. Perez-Atayde, R. Langer, *J. Pediatr. Surg.* **1988**, *23*, 3.
[9] A. A. Appel, M. A. Anastasio, J. C. Larson, E. M. Brey, *Biomaterials* **2013**, *34*, 6615.
[10] S. Y. Nam, L. M. Ricles, L. J. Suggs, S. Y. Emelianov, *Tissue Eng., Part B* **2015**, *21*, 88.
[11] K. Kim, W. R. Wagner, *Ann. Biomed. Eng.* **2016**, *44*, 621.
[12] M. E. Mertens, A. Hermann, A. Bühren, L. Olde Damink, D. Möckel, F. Gremse, J. Ehling, F. Kiessling, T. Lammers, *Adv. Funct. Mater.* **2014**, *24*, 754.
[13] M. E. Mertens, S. Koch, P. Schuster, J. Wehner, Z. Wu, F. Gremse, V. Schulz, L. Rongen, F. Wolf, J. Frese, V. N. Gesché, M. van Zandvoort, P. Mela, S. Jockenhoevel, F. Kiessling, T. Lammers, *Biomaterials* **2015**, *39*, 155.
[14] K. Kim, C. G. Jeong, S. J. Hollister, *Acta Biomater.* **2008**, *4*, 783.
[15] Y. S. Zhang, X. Cai, J. Yao, W. Xing, L. V. Wang, Y. Xia, *Angew. Chem., Int. Ed.* **2014**, *53*, 184.
[16] H. Zhou, A. Gawlik, C. Hernandez, M. Goss, J. Mansour, A. Exner, *ACS Biomater. Sci. Eng.* **2016**, *2*, 1005.
[17] J. Yu, K. Takanari, Y. Hong, K.-W. Lee, N. J. Amoroso, Y. Wang, W. R. Wagner, K. Kim, *Biomaterials* **2013**, *34*, 2701.
[18] D. W. Park, S.-H. Ye, H. B. Jiang, D. Dutta, K. Nonaka, W. R. Wagner, K. Kim, *Biomaterials* **2014**, *35*, 7851.
[19] S. H. Kim, J. H. Lee, H. Hyun, Y. Ashitate, G. Park, K. Robichaud, E. Lunsford, S. J. Lee, G. Khang, H. S. Choi, *Sci. Rep.* **2013**, *3*, 1198.
[20] J. Fornaro, S. Leschka, D. Hibbeln, A. Butler, N. Anderson, G. Pache, H. Scheffel, S. Wildermuth, H. Alkadhi, P. Stolzmann, *Insights Imaging* **2011**, *2*, 149.
[21] M. R. Oliva, K. J. Mortele, *Cardiac PET and PET/CT Imaging*, Springer, New York **2007**, pp. 83–93.
[22] A. de Vries, E. Custers, J. Lub, S. van den Bosch, K. Nicolay, H. Grüll, *Biomaterials* **2010**, *31*, 6537.
[23] F. Mottu, D. A. Rufenacht, E. Doelker, *Invest. Radiol.* **1999**, *34*, 323.
[24] N. R. James, J. Philip, A. Jayakrishnan, *Biomaterials* **2006**, *27*, 160.
[25] M. A. B. Kruft, A. Benzina, F. Bär, F. H. van der Veen, C. W. Bastiaansen, R. Blezer, T. Lindhout, L. H. Koole, *J. Biomed. Mater. Res.* **1994**, *28*, 1259.
[26] M. A. B. Kruft, A. Benzina, R. Blezer, L. H. Koole, *Biomaterials* **1996**, *17*, 1803.
[27] S. Dawlee, A. Jayakrishnan, M. Jayabalan, *J. Mater. Sci.: Mater. Med.* **2009**, *20*, 243.
[28] Y. Yang, S. M. Dorsey, M. L. Becker, S. Lin-Gibson, G. E. Schumacher, G. M. Flaim, J. Kohn, C. G. Simon, *Biomaterials* **2008**, *29*, 1901.
[29] K. A. Aamer, K. L. Genson, J. Kohn, M. L. Becker, *Biomacromolecules* **2009**, *10*, 2418.
[30] A. L. Carbone, M. Song, K. E. Uhrich, *Biomacromolecules* **2008**, *9*, 1604.
[31] M. J. Sandker, A. Petit, E. M. Redout, M. Siebelt, B. Müller, P. Bruin, R. Meyboom, T. Vermonden, W. E. Hennink, H. Weinans, *Biomaterials* **2013**, *34*, 8002.
[32] C. Rode, A. Schmidt, R. Wyrwa, J. Weisser, K. Schmidt, N. Moszner, R. P. Gottlöber, K. Heinemann, M. Schnabelrauch, *Polym. Int.* **2014**, *63*, 1732.
[33] Y. B. J. Aldenhoff, M.-A. B. Kruft, A. Paul Pijpers, F. H. van der Veen, S. K. Bulstra, R. Kuijer, L. H. Koole, *Biomaterials* **2002**, *23*, 881.
[34] E. Wisse, A. J. H. Spiering, E. N. M. van Leeuwen, R. A. E. Renken, P. Y. W. Dankers, L. A. Brouwer, M. J. A. van Luyn, M. C. Harmsen, N. A. J. M. Sommerdijk, E. W. Meijer, *Biomacromolecules* **2006**, *7*, 3385.
[35] R. A. Koevoets, R. M. Versteegen, H. Kooijman, A. L. Spek, R. P. Sijbesma, E. W. Meijer, *J. Am. Chem. Soc.* **2005**, *127*, 2999.
[36] E. Wisse, L. E. Govaert, H. E. H. Meijer, E. W. Meijer, *Macromolecules* **2006**, *39*, 7425.
[37] P. Y. W. Dankers, M. C. Harmsen, L. A. Brouwer, M. J. A. van Luyn, E. W. Meijer, *Nat. Mater.* **2005**, *4*, 568.
[38] P. Y. W. Dankers, J. M. Boomker, A. Huizinga-van der Vlag, E. Wisse, W. P. J. Appel, F. M. M. Smedts, M. C. Harmsen, A. W. Bosman, W. Meijer, M. J. A. van Luyn, *Biomaterials* **2011**, *32*, 723.
[39] B. D. Ippel, H. M. Keizer, P. Y. W. Dankers, *Adv. Funct. Mater.* **2019**, *29*, 1805375.
[40] M. H. Bakker, C. C. S. Tseng, H. M. Keizer, P. R. Seevinck, H. M. Janssen, F. J. Van Slochteren, S. A. J. Chamuleau, P. Y. W. Dankers, *Adv. Healthcare Mater.* **2018**, *7*, 1701139.
[41] M. C. P. Brugmans, S. H. M. Söntjens, M. A. J. Cox, A. Nandakumar, A. W. Bosman, T. Mes, H. M. Janssen, C. V. C. Bouten, F. P. T. Baaijens, A. Driessen-Mol, *Acta Biomater.* **2015**, *27*, 21.
[42] E. E. van Haaften, R. Duijvelshoff, B. D. Ippel, S. H. M. Söntjens, M. H. C. J. van Houtem, H. M. Janssen, A. I. P. M. Smits, N. A. Kurniawan, P. Y. W. Dankers, C. V. C. Bouten, *Acta Biomater.* **2019**, *92*, 48.
[43] T. B. Wissing, V. Bonito, E. E. van Haaften, M. van Doeselaar, M. C. P. Brugmans, H. M. Janssen, C. V. C. Bouten, A. L. P. M. Smits, *Front. Bioeng. Biotechnol.* **2019**, *7*, 87.
[44] R. Duijvelshoff, N. C. A. van Engeland, K. M. R. Gabriels, S. H. M. Söntjens, A. I. P. M. Smits, P. Y. W. Dankers, C. V. C. Bouten, *Bioengineering* **2018**, *5*, 61.
[45] C. X. F. Lam, D. W. Hutmacher, J.-T. Schantz, M. A. Woodruff, S. H. Teoh, *J. Biomed. Mater. Res., Part A* **2009**, *90A*, 906.
[46] K. Davy, *EP0684222B1*, **1998**.
[47] A. Cipitria, A. Skelton, T. R. Dargaville, P. D. Dalton, D. W. Hutmacher, *J. Mater. Chem.* **2011**, *21*, 9419.
[48] S. Eshraghi, S. Das, *Acta Biomater.* **2010**, *6*, 2467.
[49] I. Engelberg, J. Kohn, *Biomaterials* **1991**, *12*, 292.
[50] R. Akhtar, M. J. Sherratt, J. K. Cruickshank, B. Derby, *Mater. Today* **2011**, *14*, 96.
[51] E. S. Fioretta, J. O. Fledderus, E. A. Burakowska-Meise, F. P. T. Baaijens, M. C. Verhaar, C. V. C. Bouten, *Macromol. Biosci.* **2012**, *12*, 577.
[52] W. Wu, R. A. Allen, Y. Wang, *Nat. Med.* **2012**, *18*, 1148.
[53] T. Yokota, H. Ichikawa, G. Matsumiya, T. Kuratani, T. Sakaguchi, S. Iwai, Y. Shirakawa, K. Torikai, A. Saito, E. Uchimura, N. Kawaguchi, N. Matsuura, Y. Sawa, *J. Thorac. Cardiovasc. Surg.* **2008**, *136*, 900.
[54] S. de Valence, J.-C. Tille, D. Mugnai, W. Mrówczyński, R. Gurny, M. Möller, B. H. Walpoth, *Biomaterials* **2012**, *33*, 38.
[55] W. Mrówczyński, D. Mugnai, S. de Valence, J.-C. Tille, E. Khabiri, M. Cikirikcioglu, M. Möller, B. H. Walpoth, *J. Vascul. Surg.* **2014**, *59*, 210.
[56] J. Kluin, H. Talacua, A. I. P. M. Smits, M. Y. Emmert, M. C. P. Brugmans, E. S. Fioretta, P. E. Dijkman, S. H. M. Söntjens, R. Duijvelshoff, S. Dekker, M. W. J. T. Janssen-van den Broek, V. Lintas, A. Vink, S. P. Hoerstrup, H. M. Janssen, P. Y. W. Dankers, F. P. T. Baaijens, C. V. C. Bouten, *Biomaterials* **2017**, *125*, 101.
[57] P. Zilla, D. Bezuidenhout, P. Human, *Biomaterials* **2007**, *28*, 5009.